

Ultraviolet photoemission and low-energy-electron diffraction studies of TiO_2 (rutile) (001) and (110) surfaces

R. H. Tait* and R. V. Kasowski

Central Research and Development Department, E. I. du Pont de Nemours and Company, Wilmington, Delaware 19898

(Received 18 June 1979)

We have examined the (001) and (110) faces of TiO_2 (rutile) using ultraviolet photoelectron spectroscopy (UPS), low-energy-electron diffraction (LEED), and Auger electron spectroscopy (AES). We found that the (001) surface is unstable and reconstructs or facets when annealed while the (110) surface is stable and does not reconstruct. Other indications of the relative instability of the (001) surface include the presence of a surface phase change for $T > 950^\circ\text{C}$, significant oxygen-adsorption effects, and thermal instability in the concentration of surface Ti^{3+} -O-vacancy defects.

I. INTRODUCTION

Transition-metal oxides are known to be catalytically active for a large class of thermal and photoinduced chemical processes. In particular, TiO_2 has been found to be a very efficient catalyst for the photo-oxidation of a number of organic molecules¹ and water.² In an effort to characterize the surface properties of this catalytically important material, we carried out ultraviolet-photoelectron spectroscopic (UPS) and low-energy-electron diffraction (LEED) studies of the behavior of single-crystal surfaces of TiO_2 . These studies had the objective of examining the role of surface electronic structure in determining surface stability.

We report here on a detailed UPS and LEED study of the surface properties of the (001) and (110) faces of TiO_2 . We found that the (001) surface is unstable and reconstructs or facets upon annealing while the (110) surface is thermally stable and does not undergo reconstruction. These observations are consistent with theoretical calculations of the surface density of states of TiO_2 .³ We also found that the number of surface Ti^{3+} -O-vacancy defects on high-temperature annealed (001) surfaces is sensitive to additional low-temperature heat treatments while the number of similar defects on high-temperature annealed (110) surfaces is thermally stable. By use of controlled gas treatment and annealing procedures, we have identified both weakly bound molecular oxygen and strongly bound dissociated oxygen on TiO_2 surfaces exposed to O_2 gas. The nature of the adsorbed oxygen species is strongly dependent on the nature of the adsorbing TiO_2 surface. In addition, the UPS spectra of reduced surfaces of TiO_2 (i.e., TiO_x surfaces with $x < 2$) produced by Ar^+ -ion bombardment are consistent with one-electron density-of-states (DOS) calculations for Ti_2O_3 and support the conclusion that the *local* O-Ti coordination at the surface is the major determin-

ing factor of surface band structure for TiO_2 surfaces.

Earlier works have examined other features of the surface properties of the semiconducting oxides of titanium with major emphasis on the nature of surface defects on TiO_2 and SrTiO_3 surfaces. Henrich *et al.* used UPS, LEED, and energy-loss spectroscopy (ELS) to study the behavior of surface Ti^{3+} -O-vacancy defects on the ordered (110) face of TiO_2 ,⁴ and (100) face of SrTiO_3 ,^{5,6} as well as disordered Ar^+ -bombarded TiO_2 surfaces^{4,5} and SrTiO_3 surfaces.^{5,6} They found that the bombarded (100) surface of SrTiO_3 and the bombarded (110) surface of TiO_2 , as well as the annealed bombarded (100) surface of SrTiO_3 , contained many such surface defects, while the annealed (110) surface of TiO_2 and the vacuum fractured (100) surface of SrTiO_3 contained very few. They also observed that these surface defects are sensitive to oxygen exposure, and they identified the presence of adsorbed O^{2-} on some surfaces. Finally, they found that the (110) face of TiO_2 and the (100) face of SrTiO_3 do not reconstruct following annealing.

Chung, Lo and Somorjai⁷ have presented results on the surface properties of the (110), (100), and (001) faces of TiO_2 . They reported that the annealed (110) face is unreconstructed while the (100) reconstructs and the (001) face facets after annealing. They observed only a small number of surface Ti^{3+} -O-vacancy defects on all of the annealed TiO_2 surfaces, but they found a large number of such defects on Ar^+ -bombarded surfaces and surfaces with titanium metal deposited on them. They reported substantial surface stoichiometry changes (i.e., loss of oxygen) for ordered (100) surfaces of TiO_2 as a function of annealing temperatures for $T > 600^\circ\text{C}$. They also found that different treatments of these TiO_2 surfaces (i.e., Ar^+ -ion bombardment, O^+ -ion bombardment, deposition of titanium metal, O_2 adsorption, and annealing)

give rise to different work functions, and they argued that this implies a variation in band bending. Finally, they concluded that surface structure, surface work function, and surface band bending effect the rate of the photoreactivity of TiO_2 surfaces and that a surface layer of Ti_2O_3 is the active agent in the photodecomposition of water.

Finally, Lo and Somorjai⁸ have reported results of a LEED, AES, ELS, and UPS study of the (111) face of SrTiO_3 . They found a substantial concentration of Ti^{3+} -O-vacancy defects on both Ar^+ -ion-bombarded and annealed (111) SrTiO_3 surfaces, although the defect concentration on the (111) face was substantially smaller than the defect concentration found on the (100) face.⁶ Lo and Somorjai also found that the defect concentration was temperature dependent. They concluded that a surface layer of stable defects is responsible for the high activity of SrTiO_3 for the photodecomposition of water.

In the remainder of this paper we describe in detail our findings for the disordered Ar^+ -bombarded (001) surface of TiO_2 , as well as the ordered (001) and (110) surfaces. We discuss these results in relation to one-electron DOS calculations.³ Our efforts are aimed at understanding the differences in stability of the two ordered surfaces in terms of their fundamental electronic properties. We do not concentrate solely on studying the properties of surface defects, but instead examine the overall behavior of these two surfaces. Our characterization studies of Ar^+ -ion bombarded surfaces were carried out to help understand these fundamental properties. In Sec. II we describe the experimental details of our work. In Sec. III we present our results, and in Sec. IV we give a summary and our conclusions.

II. EXPERIMENTAL PROCEDURES

The (001) and (110) oriented single-crystal samples used in this study were prepared in the following manner. A single-crystal boule grown by flame fusion was aligned to within $\pm 1.5^\circ$ of the desired orientation by x-ray back reflection, and $\frac{1}{2}$ -mm-thick slices were then cut from it using a diamond embedded string saw. The slices were mechanically polished to an optical finish using various grades of polishing powders ending with 0.3- μm alumina. Following mechanical polishing, the slices were chemically etched to eliminate the surface damage layer. The (110) oriented sample was etched in molten KOH at $T = 420^\circ\text{C}$ for 30 min,⁹ and the (001) oriented sample was etched in molten

KHSO_4 at $T = 620^\circ\text{C}$ for 30 min.¹⁰ The samples were then boiled in a mixture of HNO_3 (45% vol.), HCl (45% vol.), and HF (10% vol.) for one hour⁹ to remove the residue from the chemical etch. The samples were next thoroughly rinsed with distilled water. Following cleaning, the single-crystal sample was inserted into a molybdenum crystal cup, and a molybdenum disk with a Pt-Pt: 13%-at.-Rh thermocouple attached to it was placed into the cup behind it. A standard Varian W-Re resistance heater (potted in Al_2O_3 and encased in a molybdenum container) was next inserted into the cup and firmly pressed against the molybdenum disk. This entire assembly was then mounted in a standard vacuum manipulator and inserted into the vacuum system.

To ensure uniform and controlled heating of the sample, a second W-Re heater (with a Pt-Pt: 13%-at.-Rh thermocouple attached) was installed in the vacuum chamber so that the front surface of the TiO_2 crystal could be positioned to within 1 mm of the face of this heater. All heat treatments were carried out with the temperature of both the back and front heaters controlled at the annealing temperature desired. The degree of temperature control varied from $\pm 1^\circ\text{C}$ at the lowest annealing temperature ($T = 100^\circ\text{C}$) to $\pm 6^\circ\text{C}$ at the highest annealing temperature ($T = 1100^\circ\text{C}$).

Sample treatments in addition to heating included argon-ion bombardment and exposure to O_2 . All Ar^+ -ion-bombardment treatments were carried out using a 2-KeV Ar^+ -ion beam with a current density (at the sample surface) of approximately $8 \mu\text{A}/\text{cm}^2$ and with the beam incident at an angle of about 50° to the sample normal. All Ar^+ -ion-bombardment treatments (except where explicitly stated otherwise) lasted 30 min. During oxygen exposures gas pressure was monitored using a low-current ionization gauge to minimize ionization-gauge effects.

After inserting the sample into the vacuum system, Ar^+ -ion-bombardment and high-temperature ($T = 800$ – 900°C) heating cycles were used to clean the sample and to bulk reduce it. Residual carbon and potassium contamination found on some of the sample surfaces was readily removed by this treatment. Bulk reduction of the sample (corresponding to 10^{18} – 10^{19} oxygen vacancies per cm^3) (Ref. 11) was caused by this procedure as evidenced by the dark blue color of the sample following treatment.

All experiments were carried out in a baked, ion-pumped, ultrahigh vacuum system which had a base pressure of 5×10^{-11} Torr and a typical operating pressure of 2×10^{-10} Torr. The system bakeout ($T = 200^\circ\text{C}$ for eight hours) proved necessary for valid characterization of some TiO_2 surfaces (in particular Ar^+ -ion-bombarded surfaces)

as the impurities present in the unbaked vacuum system (particularly H_2O) readily absorbed on these surfaces and gave rise to extraneous features in the UPS spectra.

UPS measurements were made using a retarding field electron energy analyzer with an energy resolution of 0.2 eV (as determined from examination of the Fermi edge of a clean Pt foil) and a sweep rate of 1.3 eV/min. UPS data were collected digitally using a signal averager for later processing. The photoexcitation light beam was incident at an angle of 45° to the sample surface normal, and all electrons emitted in a 45° angle cone about the normal to the sample surface were detected by the electron energy analyzer.

The light source used for the photoemission measurements was a differentially pumped He I resonance lamp employing a microwave powered electrodeless discharge. Commercially available ultrapure helium gas (<1 ppm total impurities) was used without further purification. Under normal operating conditions (65 W of microwave power and a pressure of approximately 0.8 Torr in the discharge region) the intensity of the secondary He I β line (23.09 eV) produced by our resonance lamp was 2.9% of the intensity of the main He I α line (21.22 eV). All UPS data shown have been corrected for this "ghost" line.

A standard 4-grid LEED system was used for retarding field Auger analysis as well as LEED analysis. In the LEED mode, electron beam energies of 20–160 eV and beam currents of 0.1–3.0 μA were used. In the Auger mode, an electron beam energy of 1600 eV and a beam current of 30 μA were used with a beam diameter of about 0.5 mm. All Auger measurements were made using a modulation voltage of 5 V peak to peak, and all Auger intensities reported here are based on measurements of peak-to-peak intensity of the relevant transitions.

With the current density used in the Auger mode (15 mA/cm²) we found significant electron-beam-induced reduction of some of the TiO_2 surfaces. For example, following eight min of electron bombardment of an annealed (001) surface, we observed a 10% decrease in the intensity of the oxygen Auger peak at 510 eV while the titanium peaks at 381 and 416 eV were unaffected. Therefore, to minimize electron beam effects we scanned the O (510 eV) Auger peak first for all Auger measurements reported here.

III. RESULTS AND DISCUSSION

A. Ar^+ -ion-bombarded surfaces

As part of our characterization studies of the annealed (001) and (110) surfaces of TiO_2 , we

have also examined some of the properties of the Ar^+ -ion-bombarded (001) surface of TiO_2 . Lengthy Ar^+ -ion bombardment of an ordered TiO_2 sample reduces the surface (because of preferential sputtering of oxygen) to a depth greater than the Auger electron escape depth as well as disordering it.^{4,7} We have found that a fair amount of insight into the nature of surface defects and adsorbed oxygen species on the annealed surfaces was gained by studying reduced and disordered TiO_2 surfaces. We also found that the change in the valence-band density of states which occurs as TiO_2 becomes reduced during bombardment is consistent with our theoretical DOS calculations.³

In Fig. 1 we show the UPS spectrum of a TiO_2 (001) surface that had been Ar^+ -ion bombarded for 30 min. This spectrum is essentially identical to the spectrum from an Ar^+ -ion bombarded- (110) surface of TiO_2 ,⁴ and seems to be characteristic of clean, disordered, and reduced TiO_2 surfaces.¹² It has been shown that the UPS spectrum of bombarded TiO_2 is comparable to the spectrum of vacuum fractured Ti_2O_3 ,⁴ and the observed O(510 eV) to Ti(380 eV) Auger ratio [1.22 for a 30 min Ar^+ -bombarded- (001) surface versus 1.74 for an annealed (001) surface] is consistent with this assignment of the surface stoichiometry. Therefore, we have included in Fig. 1 our calculated occupied one-electron DOS for bulk Ti_2O_3 .³ As can be seen from the figure, the most prominent features in the experimental data (a small and

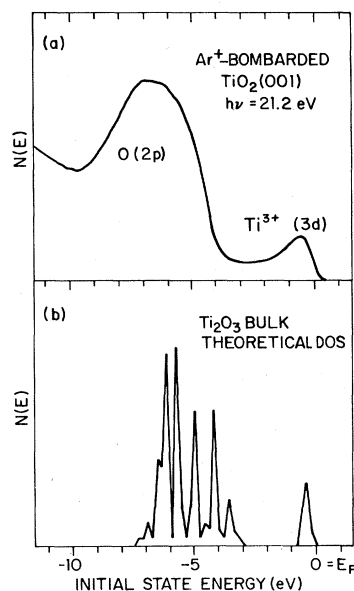


FIG. 1. (a) Photoemission spectra of an Ar^+ -bombarded TiO_2 (001) surface. (b) Theoretical one-electron density of states (DOS) of bulk Ti_2O_3 (see Ref. 3).

relatively narrow peak centered at -0.7 eV and a broad peak with a maximum at -6.8 eV are reasonably well reproduced by the theoretical DOS.

The basic form of the band structure of Ti_2O_3 (and hence also of Ar^+ -bombarded TiO_2) is typical of that for the oxides of titanium from TiO_2 to TiO .^{3,13} This band structure is characterized by a predominantly $\text{O}(2p)$ derived band (typically 6 eV wide and centered near -6 eV) separated by a gap (typically 3 eV) from a predominantly $\text{Ti}(3d)$ derived band. The location of the Fermi level for a given oxide depends on the oxygen to titanium stoichiometry (and hence the average valence state of the titanium) and varies from just below the $\text{Ti}(3d)$ band edge for slightly reduced n -type TiO_2 (i.e., $\sim 10^{19}$ O vacancies per cm^3) to about 1.7 eV into the $\text{Ti}(3d)$ band for TiO .¹³

While the general form of the band structure is preserved, the details of the valence-band density of states [in particular the shape of the $\text{O}(2p)$ derived band] change substantially in going from one stoichiometry to another, as for example in going from TiO_2 to TiO_x with $x \sim 1.5$. We have studied this transition by measuring the UPS spectra of a (001) surface following Ar^+ -ion bombardment for different lengths of time. In Fig. 2 we show the spectrum from an ordered (001) surface of TiO_2 that had not been bombarded, as well as spectra from the same (001) surface after Ar^+ -ion bombardment for times varying from 30 sec to 5 min. All of the bombarded surfaces were completely disordered as none of them exhibited

LEED patterns following treatment. In our discussion of these results we will concentrate on the details of the $\text{O}(2p)$ derived band, since Henrich *et al.*⁴ have already discussed the behavior of the $\text{Ti}^{3+}(3d)$ emission peaks.

For the ordered (001) surface of TiO_2 (which we will discuss in more detail in the next section), the $\text{O}(2p)$ derived portion of the spectrum is characterized by a large peak at -5.2 eV accompanied by a smaller peak (or shoulder) at -7.8 eV. When this surface is reduced and disordered by bombardment, a new peak appears at -6.8 eV which obscures the peak (or shoulder) at -7.8 eV. As bombardment continues, the peak at -6.8 eV grows in intensity while the peak at -5.2 eV steadily shrinks. The growth of the new peak at -6.8 eV coincides with the decrease in the surface O to Ti Auger ratio which goes from 1.74 for the annealed surface to 1.31 for the surface after 5 min of bombardment. After this period, the surface has nearly reached its steady state composition (which we have said corresponds approximately to Ti_2O_3), and further bombardment does not change the UPS spectrum. For this surface the only prominent $\text{O}(2p)$ feature is a broad peak with a maximum at -6.8 eV.

In Fig. 3 we show the calculated filled DOS for both bulk TiO_2 and bulk Ti_2O_3 .³ The major change that takes place in the $\text{O}(2p)$ portion of the UPS spectrum for the (001) surface as it is reduced (namely the shift of the dominant peak in the spec-

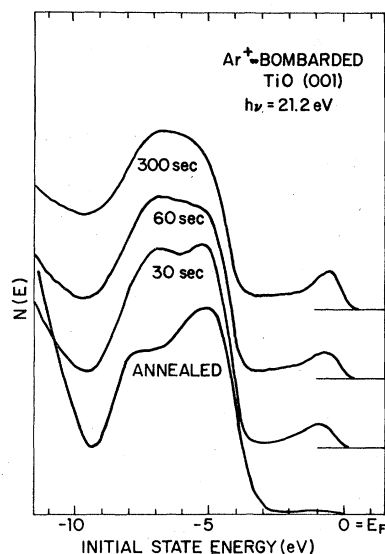


FIG. 2. Photoemission spectra of annealed TiO_2 (001) surfaces that had been bombarded for varying lengths of time. Bombardment times are shown in the figure.

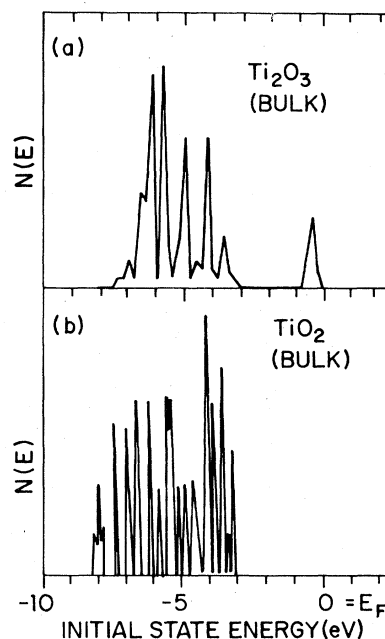


FIG. 3. Theoretical occupied one-electron density of states (DOS) for (a) bulk Ti_2O_3 , and (b) bulk TiO_2 .

tra from -5.2 to -6.8 eV) is mirrored in the theoretical DOS. The height of the peak at -6.0 eV in the calculated DOS is related to the amount of $O(2p)$ - $Ti(3d)$ hybridization present,³ which is dependent on the local coordination of O atoms by Ti atoms in the solid. Therefore, the -6.0 eV peak in the theoretical DOS for Ti_2O_3 is larger than the same peak in TiO_2 simply because the O atoms are coordinated by three Ti atoms in TiO_2 and four Ti atoms in Ti_2O_3 . The systematic increase in the height of the lower initial energy UPS peak as reduction of the surface proceeds simply reflects this changing coordination.

We have studied the interaction of oxygen with an Ar^+ -ion-bombarded (001) surface. In Fig. 4 we show UPS spectra for a bombarded (001) surface following exposures to O_2 varying from 1.6 to 1.3×10^7 L (1 langmuir = 10^{-6} Torr sec). The transformation in the spectra that takes place as the magnitude of oxygen exposure ϕ increases is essentially the inverse of the transformation that occurs when an ordered surface is bombarded: i.e., the magnitude of the $Ti^{3+}(3d)$ emission decreases continuously and the maximum in the $O(2p)$ band shifts from -6.8 to -5.2 eV. Also, the O to Ti Auger ratio varies from 1.22 to 1.56 . The changes in the UPS spectra observed for a bombarded (001) surface following O_2 exposure are comparable to the changes seen in the spectra of a bombarded (110) surface following exposure to O_2 .^{4,5}

A more detailed picture of the rate of oxidation

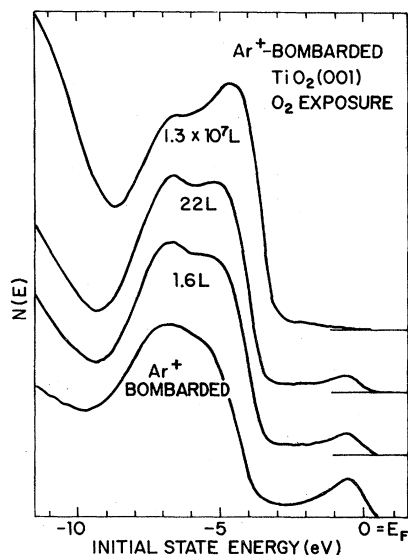


FIG. 4. Photoemission spectra of Ar^+ -bombarded TiO_2 (001) surfaces following different oxygen exposures. Exposures are indicated on the figure.

of the bombarded (001) surface was obtained by measurement of the height of the $Ti^{3+}(3d)$ peak as a function of oxygen exposure. In Fig. 5 we plot these data. For exposures $\phi < 2 \times 10^3$ L, the peak amplitude was monitored continuously as a function of exposure by fixing the retarding voltage of the electron energy analyzer at this peak energy. For exposures $\phi > 2 \times 10^3$ L, full UPS spectra were taken, and the height of the $Ti^{3+}(3d)$ measured.

Three separate regions as a function of exposure are apparent in the data of Fig. 5: region I with $\phi \lesssim 3$ L, region II with $3 \text{ L} \lesssim \phi \lesssim 80$ L, and region III with $\phi \gtrsim 80$ L. Region I is characterized by a high initial oxygen sticking probability as indicated by the rapid decrease of the $Ti^{3+}(3d)$ peak. Also, during oxygen adsorption in region I, the entire $O(2p)$ band grows in intensity with the leading edge of the $O(2p)$ band shifting to a higher initial energy. Region II is characterized by a substantially smaller oxygen sticking probability, as well as development of a well defined double peaked form for the $O(2p)$ band. The higher initial-energy peak of the $O(2p)$ band grows more rapidly than the lower initial-energy peak. Finally, region III is characterized by an extremely slow rate of oxygen pickup [as indicated by the very slow decrease in the $Ti^{3+}(3d)$ peak]. Region III is also characterized by the continued formation of a two-peaked form for the $O(2p)$ band with the absolute integrated intensity of the $O(2p)$ band decreasing as exposure increases.

The response of oxygen-exposed bombarded surfaces to mild heating depends strongly on the extent of oxygen exposure. For exposures in region I (i.e., $\phi \lesssim 3$ L), mildly heating the sample ($T = 150^\circ\text{C}$ for 30 min) had very little effect on the UPS spectrum. In Fig. 6 we show UPS spectra of a bombarded (001) surface following exposure to 1.6 L of O_2 and the same surface after being heated

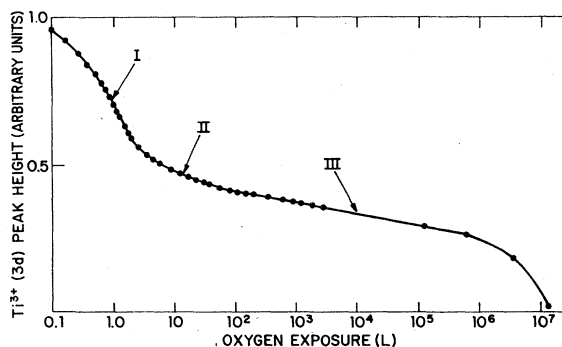


FIG. 5. Amplitude of $Ti^{3+}(3d)$ photoemission peak of an Ar^+ -bombarded TiO_2 (001) surface as a function of oxygen exposure.

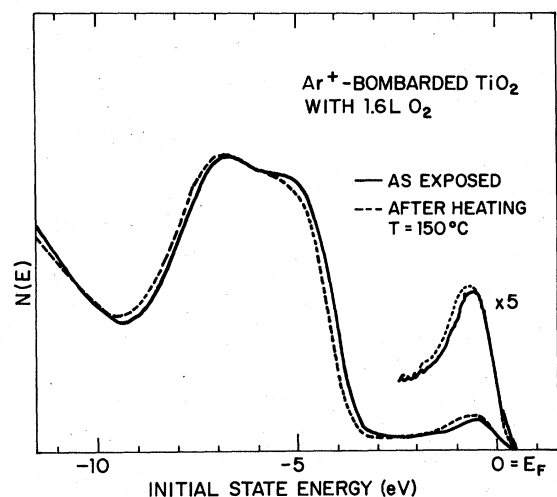


FIG. 6. Photoemission spectra of an Ar^+ -bombarded TiO_2 (001) surface first exposed to 1.6 L of O_2 and then heated to $T = 150^\circ\text{C}$ for 30 min.

at $T = 150^\circ\text{C}$ for 30 min. As can be seen, the amplitude of the $\text{Ti}^{3+}(3d)$ peak increases and the $\text{O}(2p)$ band edge shifts 0.15 eV.

Oxidized surfaces from regions II and III exhibit larger changes when similarly heated. In Fig. 7 we show spectra of a region II oxidized surface (it had been exposed to 22 L of O_2 following Ar^+ -ion bombardment) before and after being heated at $T = 150^\circ\text{C}$ for 30 min. The spectra for the heated surface has an altered $\text{O}(2p)$ band shape and also a larger $\text{Ti}^{3+}(3d)$ peak.

In Fig. 8 we show spectra of an oxidized surface from region III before and after being heated to

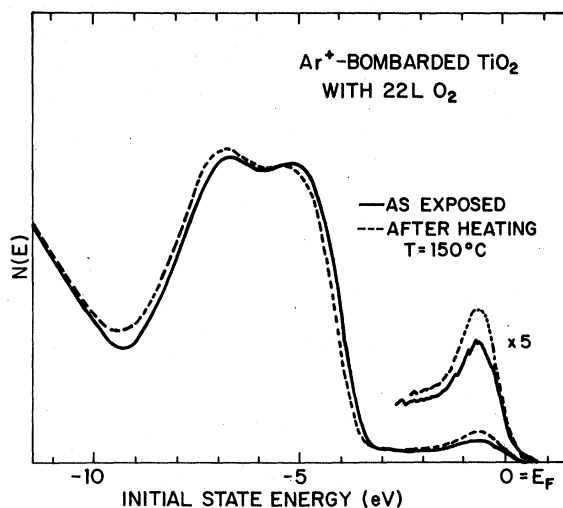


FIG. 7. Photoemission spectra of an Ar^+ -bombarded TiO_2 (001) surface first exposed to 22 L of O_2 and then heated to $T = 150^\circ\text{C}$ for 30 min.

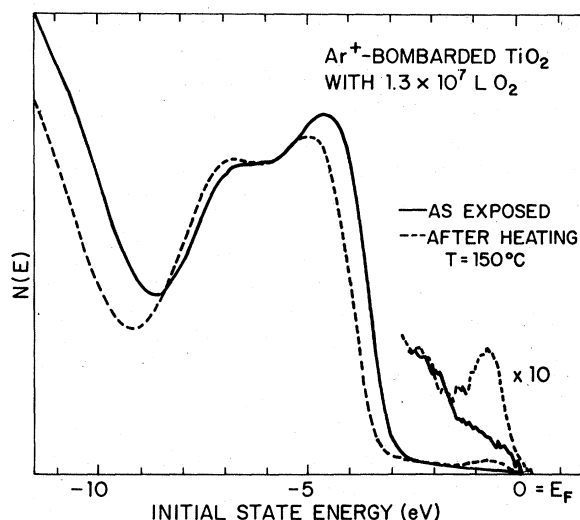


FIG. 8. Photoemission spectra of an Ar^+ -bombarded TiO_2 (001) surface first exposed to 1.3×10^7 L of O_2 and then heated at $T = 150^\circ\text{C}$ for 30 min.

$T = 150^\circ\text{C}$ for 30 min. As can be seen, the $\text{Ti}^{3+}(3d)$ emission is increased by this mild heat treatment. However, it is clear from comparison of Figs. 7 and 8 that the additional exposure (from 22 to 1.3×10^7 L) had irreversibly decreased the number of Ti^{3+} surface species since, following heating at $T = 150^\circ\text{C}$, the surface exposed to 1.3×10^7 L of O_2 still had a smaller $\text{Ti}^{3+}(3d)$ peak than the surface exposed to 22 L.¹⁴

Based on these observations, we have made the following assignments for the room temperature oxidation processes taking place on the Ar^+ -ion bombarded (001) face of TiO_2 :

Region I: $4\text{Ti}^{3+} + \text{O}_2(\text{gas}) \rightarrow 4\text{Ti}^{4+} + 2\text{O}^{2-}(\text{surface})$.

Region II: $\text{Ti}^{3+} + \text{O}_2(\text{gas}) \rightarrow \text{Ti}^{4+} + \text{O}_2^-(\text{surface})$.

Region III: $3\text{Ti}^{3+} + \text{O}_2^-(\text{surface}) \rightarrow 3\text{Ti}^{4+} + 2\text{O}^{2-}(\text{bulk})$,
 $\text{Ti}^{3+} + \text{O}_2(\text{gas}) \rightarrow \text{Ti}^{4+} + \text{O}_2^-(\text{surface})$.

Here $\text{O}_2(\text{gas})$ is a gas-phase species, $\text{O}^{2-}(\text{surface})$ and $\text{O}_2^-(\text{surface})$ are surface species, and $\text{O}^{2-}(\text{bulk})$ is a bulk species.

Our assignment of $\text{O}^{2-}(\text{surface})$ as the adsorbed oxygen species for low exposures is in agreement with the conclusion of Henrich *et al.*⁴ This assignment is based on the strong bonding of the adsorbed species, the depopulation of the $\text{Ti}^{3+}(3d)$ UPS peak (indicating charge transfer), and the shape of the $\text{O}(2p)$ band. The adsorption is irreversible, and the UPS spectra show that the change in the $\text{O}(2p)$ is additive, indicating no change in coordination of bulk oxygen atoms.

We have assigned the adsorbed oxygen species, which desorbs at $T \leq 150^\circ\text{C}$ following exposures in regions II and III to $\text{O}_2^-(\text{surface})$, based on the following observations¹⁴: First, the low desorption temperature implies a molecular, rather than an

atomic, species. Second, the disappearance of the $\text{Ti}^{3+}(3d)$ emission implies that charge transfer has taken place. Third, O_2^- has been observed on reduced TiO_2 powders with ESR, and it has been observed to desorb at $T < 150^\circ\text{C}$.¹⁵ Fourth, the 0.5 eV shift of the entire $\text{O}(2p)$ valence band to lower initial state energies that occurred following this mild heating can be readily explained in terms of the desorption of $\text{O}_2^-(\text{surface})$ and the consequent removal of band bending caused by the presence of this charged surface species.

Finally, the oxygen species found during O_2 exposures in region III, which is responsible for the irreversible decrease in the $\text{Ti}^{3+}(3d)$ UPS peak, we have assigned to be $\text{O}^{2-}(\text{bulk})$. We base this assignment on the following observations: First, the decrease in the Ti^{3+} population implies charge transfer. Second, the changes in the $\text{O}(2p)$ band with increased exposure are nonadditive in nature (since there is a decrease in the lower binding-energy peak with increased oxygen exposure), indicating that changes in the symmetry of bulk O's are occurring. Third, the form of the $\text{O}(2p)$ band is shifting from that characteristic of Ti_2O_3 to that characteristic of TiO_2 with the growth of the peak at -5.2 eV indicating changes in bulk stoichiometry. The fact that there is still a $\text{Ti}^{3+}(3d)$ UPS peak for a bombarded surface exposed to 1.3×10^7 L of O_2 [after removal of adsorbed $\text{O}_2^-(\text{surface})$] is consistent with the Auger observation that this surface still does not have the O to Ti ratio characteristic of an annealed TiO_2 surface, and shows that diffusion of surface oxygen into the reduced bulk proceeds very slowly at room temperature.

All of our observations of the variations of the UPS spectra that occurred for TiO_2 surfaces as x varied support our conclusion that the local O-Ti coordination (as determined by the local O-Ti stoichiometry) is responsible for the band structure of these surfaces. In particular, changes in the amplitude of the -6.8 and -5.2 eV peaks in the $\text{O}(2p)$ band followed changes in the bulk stoichiometry quite closely with the presence of the -6.8 eV peak indicating deviations from the threefold Ti coordination of O atoms found in bulk TiO_2 . We will make use of this conclusion concerning the relationship between local O-Ti coordination and surface band structure in our discussion of the UPS spectra of annealed and ordered surfaces of TiO_2 .

B. TiO_2 (001)

Our one-electron DOS calculations³ for the unreconstructed (001) surface of TiO_2 show that such a surface possesses a large density of occu-

pied $\text{O}(2p)$ states in the bulk band gap. No simple contraction or expansion of surface atoms will eliminate these high initial energy states. These surface states which have been associated with dangling bonds are due to the fourfold oxygen-coordinated Ti^{4+} ions present on the unreconstructed (001) face. If we assume that the presence of such occupied band-gap states indicates that the unreconstructed surface is thermodynamically unstable, then we are led to the conclusion that the (001) surface itself should reconstruct when annealed. Our experimental findings support this conclusion.

To begin our discussion of the experimentally observed behavior of the (001) face of TiO_2 , we will describe the surface ordering and reoxidation (because of diffusion of lattice oxygen from the bulk to the surface) that occurs when a bombarded (001) surface is annealed in vacuum. In Fig. 9 we show valence-band UPS spectra for Ar^+ -ion-bombarded (001) surfaces of TiO_2 that had been annealed for 30 min at different temperatures and then allowed to cool to room temperature before examination. (All spectra shown are for surfaces that had been bombarded immediately prior to annealing.) As can be seen, the gross changes in the form of the valence band upon annealing an Ar^+ -bombarded surface are essentially the inverse of the changes seen following bombardment of an annealed surface: (1) the maximum of the $\text{O}(2p)$ band shifts from lower initial energies to higher initial energies, and (2) the $\text{Ti}^{3+}(3d)$ peak shrinks in size.

A more detailed picture of the annealing behavior of the (001) surface is shown in Fig. 10, where we have plotted both the O to Ti Auger ratio and the

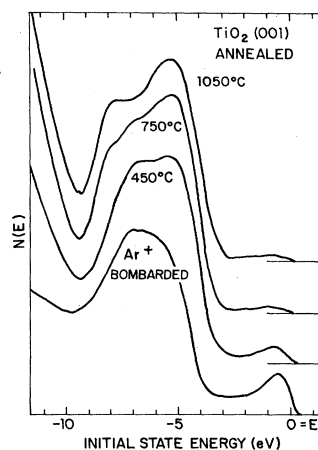


FIG. 9. Photoemission spectra of TiO_2 (001) surfaces annealed for 30 min. at different temperatures. All spectra shown are for samples Ar^+ -bombarded just prior to being annealed. Annealing temperatures are indicated on the figure.

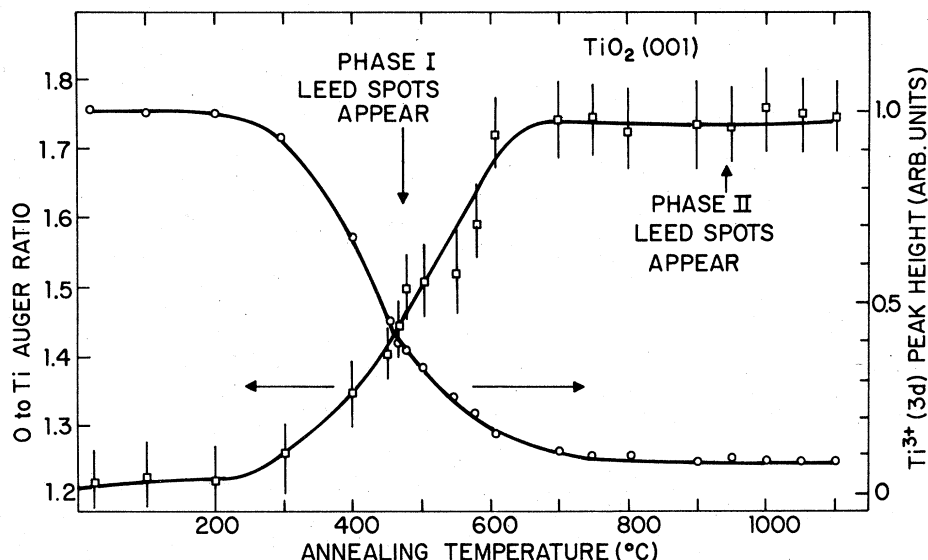


FIG. 10. Temperature dependence of the reoxidation (by diffusion of bulk lattice oxygen to the surface) of reduced and disordered TiO_2 (001) surfaces. Shown in the figure are the amplitude of the Ti^{3+} (3d) photoemission peak and the O to Ti Auger ratio of Ar^+ -bombarded TiO_2 (001) surfaces following annealing for 30 min.

amplitude of the Ti^{3+} (3d) UPS peak as a function of the annealing temperature. Clearly, surface stoichiometry changes very little for $T < 300^\circ\text{C}$ and essentially all of the stoichiometry change resulting from diffusion of lattice oxygen from the bulk to the surface is complete for $T > 600^\circ\text{C}$. Also, the depopulation of the Ti^{3+} (3d) emission peak takes place over essentially the same temperature range as the change in surface stoichiometry. LEED spots first appear at $T = 475^\circ\text{C}$, i.e., in the middle of this temperature range. Furthermore, we found a structural transformation (as shown by LEED) of the (001) surface takes place in the temperature range $T = 950\text{--}1050^\circ\text{C}$. This structural transfor-

mation takes place slowly and domains of both structures were found to coexist in this temperature range. This transformation is also irreversible, and the low-temperature phase can only be reproduced by annealing a surface that has been once again bombarded.

We also found that the lower-temperature phase (which we have labeled Phase I) of the (001) surface of TiO_2 is reconstructed or faceted in a complex way.⁷ In Fig. 11 we show a LEED pattern for this surface. While the LEED pattern has the fourfold symmetry of the unreconstructed surface and has spots at the proper location for the integral order beams, a large number of nonintegral beams are also present and many (but not all) of the LEED spots move nonradially with changes in electron energy. The spot motions that do occur with changing electron beam energy are in the [110] and [100] directions.⁷ Combined with the complexity of the patterns, this observation indicates that any new faceted surfaces present are probably reconstructed (111) or (101) surfaces. The exact nature of the surface rearrangement implied by Fig. 11 is not obvious, and at the present time, no detailed model exists of the surface geometry of a Phase I TiO_2 (001) surface. However, the presence of such a complex surface reconstruction does indicate the instability of this surface.

In Fig. 12 we show the UPS spectrum of a fully annealed Phase I (001) surface. The $\text{O}(2p)$ valence band is characterized by a triplet structure with peaks at -5.2 , -6.9 , and -7.9 eV. The leading edge of the valence band is located at -3.2 eV. A



FIG. 11. LEED pattern from a Phase II TiO_2 (001) surface. This surface had been annealed for 30 min. at $T = 750^\circ\text{C}$ following Ar^+ bombardment.

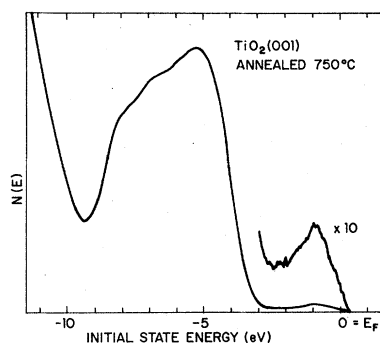


FIG. 12. Photoemission spectrum of a Phase I TiO_2 (001) surface. The surface had been annealed for 30 min. at $T = 750^\circ\text{C}$ following Ar^+ bombardment.

small residual concentration of Ti^{3+} -O-vacancy surface defects gives rise to a small $\text{Ti}^{3+}(3d)$ UPS peak at -1.0 eV.

The first observation we make concerning this spectrum is that there is no evidence of the $\text{O}(2p)$ dangling-bond surface states predicted by our DOS calculations³ for the unreconstructed (001) surface. In particular, the observed separation of the leading edge of the surface valence band from the Fermi energy is essentially identical to the bulk band gap, indicating no occupied surface $\text{O}(2p)$ states in the gap. We therefore propose that the (001) surface of TiO_2 reconstructs or facets during annealing to eliminate these energetically unfavorable states.

Next, we note that the triplet structure of the $\text{O}(2p)$ band is characteristic of reconstructed and faceted surfaces,⁷ while the unreconstructed annealed TiO_2 (110) surface (which we will discuss in detail later) exhibits a well defined doublet with peaks only at -5.2 and -7.7 eV.^{4,7} As will be shown later, the detailed shape of the central portion (i.e., that portion in the vicinity of -7 eV) of the $\text{O}(2p)$ band of ordered (001) surfaces is sensitive to surface crystal structure and surface treatment. We therefore conclude that the additional feature at -6.9 eV in the middle of the $\text{O}(2p)$ band in Fig. 12 is characteristic of surfaces having oxygen-bonding geometries deviating from that found in bulk TiO_2 .

Finally, we note that the finite concentration of Ti^{3+} -O-vacancy surface defects [as indicated by the presence of the small $\text{Ti}^{3+}(3d)$ UPS peak] found on fully annealed Phase I (001) surfaces is comparable to that seen on other TiO_2 surfaces.^{4,7} These defects have been found on all annealed TiO_2 surfaces^{4,7} and do not seem to be removed by heat treatment alone. The mechanism responsible for stabilizing these defects is not understood at present, although it is reasonable to assume that the observed surface defect concentration is simply

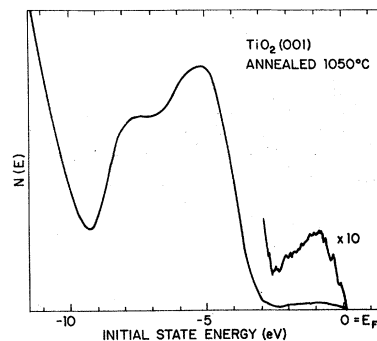


FIG. 13. Photoemission spectrum of a Phase II TiO_2 (001) surface. The surface had been annealed for 30 min. at $T = 1050^\circ\text{C}$ following Ar^+ bombardment.

the equilibrium surface defect concentration given the presence of a bulk defect concentration.

We found that the higher-temperature phase of the (001) surface (which we have labeled Phase II) differs significantly from the lower-temperature phase in both surface band structure and surface crystal structure, although Auger spectroscopy indicates no difference (to within the uncertainty in the measurement of about $\pm 4\%$) in surface stoichiometry (see Fig. 10). In Fig. 13 we show the UPS spectrum of a fully annealed Phase II surface. The $\text{O}(2p)$ band is now a doublet with peaks at -5.2 and -7.7 eV (i.e., the feature at -6.9 eV is no longer present), while the $\text{Ti}^{3+}(3d)$ peak remains essentially unchanged. In Fig. 14 we show some LEED patterns for a Phase II surface. These LEED patterns can be indexed and show that this surface is composed of a number of different domains whose LEED patterns all have symmetries of the form $(n/\sqrt{2}) \times 1 [R(\pm 45^\circ)]$. We found domains with $n = 4, 5$, and 8 coexisting on Phase II surfaces, and we also found that there was no longer evidence of faceting. No model exists at present of either the surface crystal structure of Phase II (001) surfaces or the exact nature of the structural changes occurring in the Phase I to Phase II transformation, but the existence of such a transformation is another indication of the instability of this surface.

The surface band structure of Phase II surfaces (as measured by UPS) can be changed by additional thermal treatment in a narrow temperature range. In Fig. 15 we show the UPS spectra of a Phase II (001) surface before and after reheating in vacuum at $T = 550^\circ\text{C}$ for 30 min. As can be seen, there is a substantial increase (about a factor of 2) in the amplitude of the $\text{Ti}^{3+}(3d)$ peak as well as a minor change in the form of the $\text{O}(2p)$ band following this treatment, although no significant changes in LEED pattern or O to Ti Auger ratio were observed. Treatment at lower temper-

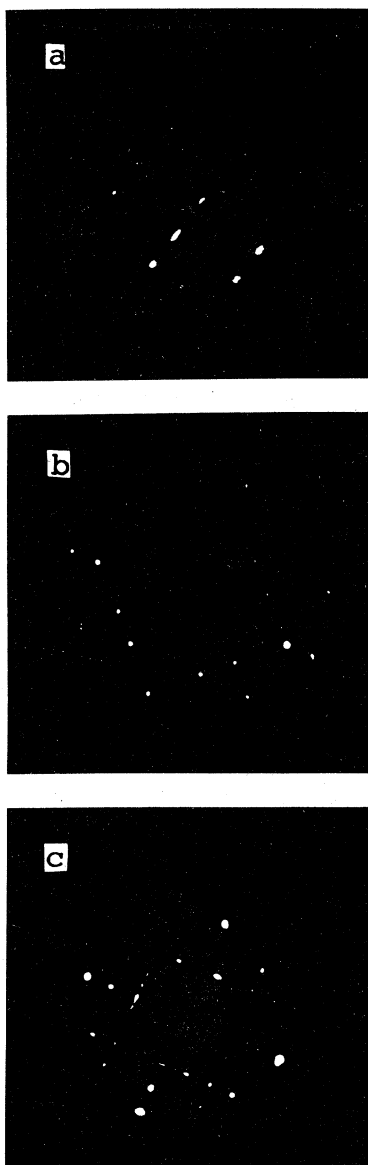


FIG. 14. LEED patterns for a Phase II TiO_2 (001) surface. The surface had been annealed at $T = 1050^\circ\text{C}$ for 30 min. (a) $E_p = 19\text{ V}$, (b) $E_p = 28\text{ V}$, and (c) $E_p = 43\text{ V}$.

atures ($T < 500^\circ\text{C}$) or higher temperatures ($T > 600^\circ\text{C}$) did not give rise to this effect. We propose that the change in surface concentration of Ti^{3+} -O-vacancy defects implied by this change in the UPS spectrum arises from the basis instability of the (001) surface.

Phase II (001) surfaces exhibit substantial oxygen adsorption effects as shown by UPS. In Fig. 16 we show the UPS spectra of a Phase II surface before and after exposure to 10^3 L of O_2 . We note three significant changes in the nature of the spectrum

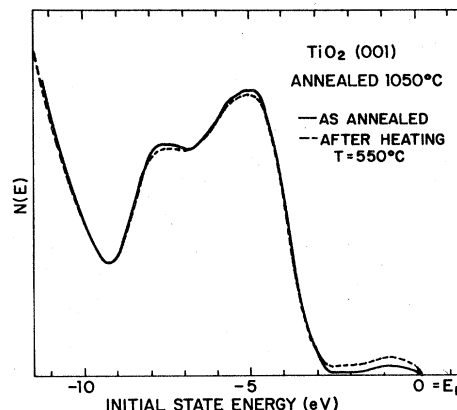


FIG. 15. Photoemission spectra of a Phase II TiO_2 (001) surface before and after reheating at $T = 550^\circ\text{C}$ for 30 min.

following this exposure: (1) the $\text{Ti}^{3+}(3d)$ peak has been completely depopulated, (2) the entire $\text{O}(2p)$ valence band has been shifted 0.2 eV closer to the Fermi energy, and (3) there has been a substantial increase in the $\text{O}(2p)$ band emission, particularly in the center of the band near -7 eV . No significant change was observed in the O to Ti Auger ratio¹⁴ or in the symmetry of the LEED pattern following oxygen exposure, although an increase in the background LEED intensity was seen.

Low-temperature heat treatment of this oxygen-exposed surface causes additional changes. In Fig. 17, we show the UPS spectra of an oxygen-exposed (1000 L) Phase II surface before and after being heated in vacuum at $T = 150^\circ\text{C}$ for one half

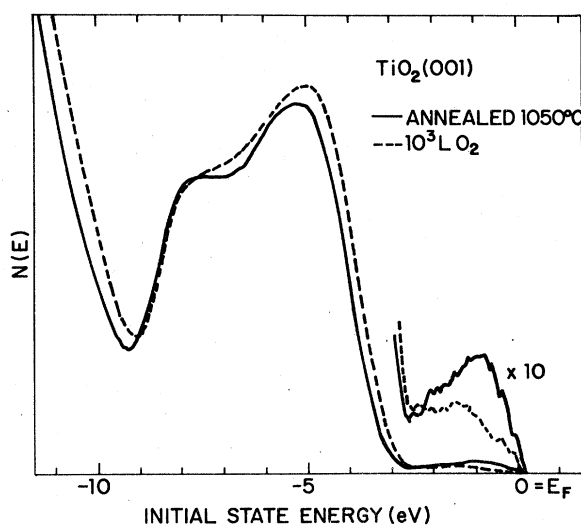


FIG. 16. Photoemission spectra of a Phase II TiO_2 (001) surface before and after exposure to 10^3 L of oxygen.

hour. As is apparent, this heat treatment causes the $\text{Ti}^{3+}(3d)$ peak to reappear and the $\text{O}(2p)$ valence band to shift 0.2 eV back to its original position. We found that additional oxygen exposures of 10^3 L and low-temperature vacuum heat treatments at $T = 150^\circ\text{C}$ simply took the spectrum between the two forms shown in Fig. 17. Only annealing in vacuum at $T > 800^\circ\text{C}$ decreased the additional $\text{O}(2p)$ emission in the center of the band.

Based on the same arguments used to explain the oxidation of Ar^+ -ion-bombarded surfaces, we have assigned the weakly bound oxygen species to be $\text{O}_2^-(\text{surface})$. Charge transfer from a Ti^{3+} -O-vacancy surface defect to an O_2 molecule to form $\text{O}_2^-(\text{surface})$ depopulates this state but does not eliminate the vacancy. Therefore, desorption of the molecular oxygen results in repopulation of the defect state and reappearance of the $\text{Ti}^{3+}(3d)$ peak. Furthermore, the 0.2 eV shift in the $\text{O}(2p)$ band following oxygen adsorption is easily attributed to band bending at the surface arising from charge transfer from a *bulk* Ti^{3+} -O-vacancy defect to a *surface* oxygen molecule yielding $\text{O}_2^-(\text{surface})$ and a depletion layer.

The strongly bound adsorbed oxygen species, which is not affected by low temperature heat treatment, we believe is dissociated oxygen, and we base this conclusion mainly on the strength of the bonding. We argue that a lack of bulk symmetry for this surface atomic oxygen species is responsible for its $\text{O}(2p)$ emission being concentrated in the middle and leading peak of the $\text{O}(2p)$ band. It is not clear what the binding site for these atomic species is. However, the existence of this

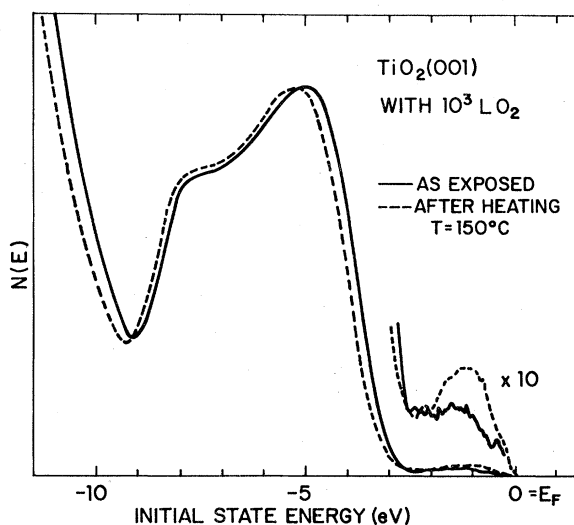


FIG. 17. Photoemission spectra of a Phase II TiO_2 (001) surface first exposed to 10^3 L of oxygen and then heated at $T = 150^\circ\text{C}$ for 30 min.

species on the (001) surface but not on the (110) (as we will discuss below) is another indication of the relative instability of the (001) surface.

C. TiO_2 (110)

Our one-electron DOS calculations³ indicate that the unreconstructed (110) surface of TiO_2 has a small number of occupied $\text{O}(2p)$ states in the bulk band gap. However, calculations based on a slight inward relaxation (0.13 \AA) of those O atoms that pucker out of the surface remove these states. If we assume that $\text{O}(2p)$ dangling-bond surface states are the underlying cause of instabilities for TiO_2 surfaces, we conclude that the (110) surface of TiO_2 should be more stable than the (001) surface. Our experimental findings as well as the findings of others^{4,7} support this conclusion.

To begin our discussion of the experimentally observed behavior of the (110) face of TiO_2 , we will describe the reoxidation and ordering that occurs when a bombarded (110) surface is annealed in vacuum. In Fig. 18 we show valence-band UPS spectra of bombarded (110) surfaces of TiO_2 that had been annealed for 30 min at different temperatures. (All spectra shown are for surfaces that were bombarded immediately prior to annealing.) The basic changes that occur in the UPS spectra as annealing proceeds are comparable to the changes seen for bombarded (001) surfaces:

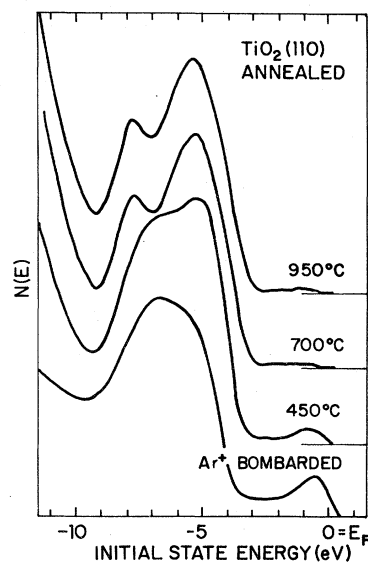


FIG. 18. Photoemission spectra of TiO_2 (110) surfaces annealed for 30 min. at different temperatures. All spectra shown are for samples Ar^+ -bombarded just prior to being annealed. Annealing temperatures are shown on the figure.

(1) the maximum of the $O(2p)$ band shifts to a higher initial state energy, and (2) the $Ti^{3+}(3d)$ peak shrinks in size.

More detail on the temperature dependence of the annealing behavior is shown in Fig. 19 where we have plotted the O to Ti Auger ratio and the $Ti^{3+}(3d)$ peak height as a function of annealing temperature. Comparison of Fig. 19 with the corresponding data for the (001) surface (see Fig. 10) shows that the critical temperature range for reoxidation of the (110) surface by diffusion of lattice oxygen from the bulk is essentially the same ($300^\circ C \leq T \leq 600^\circ C$) as that for the (001) surface. Also recognizable LEED spots appear at the same temperature ($T = 475^\circ C$) for both surfaces.

However, once annealed the (110) surface behaves differently from the (001) surface. First, the (110) surface does not reconstruct upon annealing. In Fig. 20 we show a typical LEED pattern for the (110) surface. The LEED pattern shown is for a surface annealed at $T = 900^\circ C$ for one half hour and is the (1×1) pattern indicative of an unreconstructed surface. The (110) surface does not undergo surface structural transformation comparable to that found for the (001) surface since the (1×1) LEED pattern was the only one observed.

We also found that the valence-band UPS spectra of (110) surfaces do not exhibit the variations shown by comparable spectra for (001) surfaces. In Fig. 21 we show the valence-band UPS spectrum of an ordered (110) surface of TiO_2 . The $O(2p)$ is a well defined doublet with peaks at -5.2 and -7.8 eV, and there is a small $Ti^{3+}(3d)$ peak at -1.0 eV. Furthermore, this valence-band spectrum is

characteristic of all fully ordered (110) surfaces annealed at $T \geq 650^\circ C$ and is unaffected by further heat treatments once formed. We conclude that the surface band structure of the (110) surface is stable once formed.

Finally, we found that when exposed to 10^3 L of gaseous O_2 , an ordered (110) surface adsorbs only weakly bound $O_2^-(\text{surface})$. In Fig. 22 we show the UPS spectra for an annealed (110) surface before and after exposure to 10^3 L of O_2 . In Fig. 23 we show the UPS spectra of this oxygen-exposed surface before and after heating in vacuum at $T = 150^\circ C$ for 30 min. As can be seen from Fig. 22, O_2 exposure depopulates the $Ti^{3+}(3d)$ peak and causes a substantial shift (0.4 eV) and distortion of the $O(2p)$ band. However, Fig. 23 shows that mild heating returns the $O(2p)$ band to its previous position and shape, as well as repopulating the $Ti^{3+}(3d)$ state. As for the (001) surface, we argue that the depopulation of the $Ti^{3+}(3d)$ state and the shift of the $O(2p)$ band arise from charge transfer from both surface and bulk Ti^{3+} -O-vacancy defects to form $O_2^-(\text{surface})$ and a depletion layer. Distortions of the $O(2p)$ band, we conclude, arise from the presence of the charged $O_2^-(\text{surface})$ layer on the surface. Desorption of the molecular oxygen repopulates the defect states and returns the spectrum to its original form. No sign of strongly bound adsorbed atomic oxygen is observed on the (110) surface exposed to 10^3 L of O_2 .

IV. SUMMARY AND CONCLUSIONS

We have examined the annealing and oxygen adsorption behavior of disordered (and reduced)

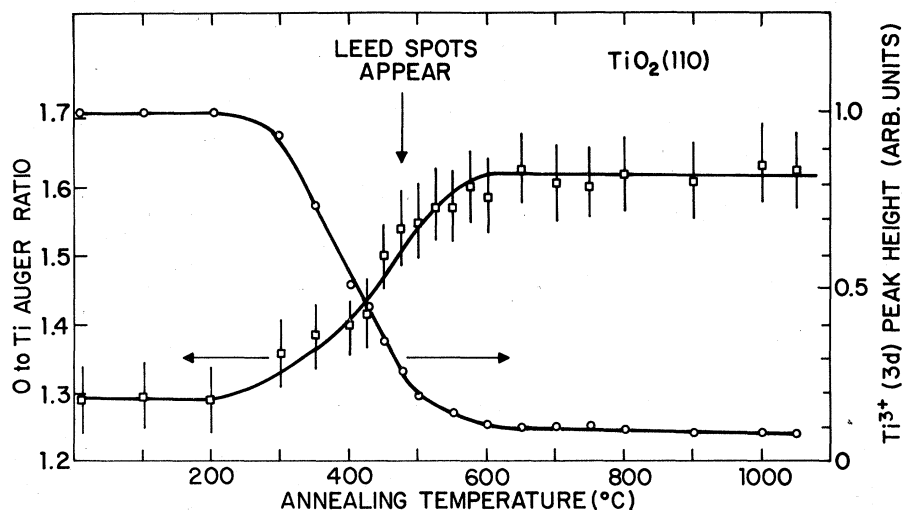


FIG. 19. Temperature dependence of the reoxidation (by diffusion of bulk lattice oxygen to the surface) or reduced and disordered TiO_2 (110) surfaces. Shown in the figure are the amplitude of the $Ti^{3+}(3d)$ photoemission peak and the O to Ti Auger ratio of Ar^+ -bombarded TiO_2 (110) surfaces following annealing for 30 min.

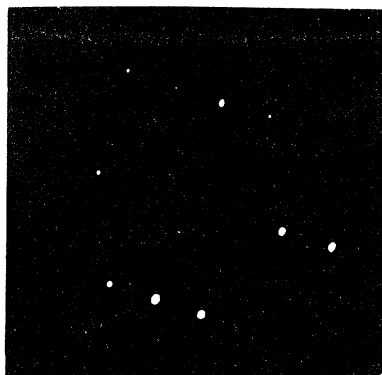


FIG. 20. LEED pattern of a TiO_2 (110) surface that had been annealed at $T = 950^\circ\text{C}$ for 30 min. after Ar^+ bombardment.

Ar^+ -ion-etched surfaces of TiO_2 as well as ordered (001) and (110) surfaces of TiO_2 . We found that the experimentally observed changes in the valence-band electronic structure of ordered TiO_2 surfaces, when they were reduced from TiO_2 to TiO_x (with $x \sim 1.5$), are well accounted for qualitatively by our one-electron DOS calculations³ and can be attributed to the changing oxygen coordination of titanium atoms. Furthermore, we have identified three different adsorbed oxygen species [$\text{O}^{2-}(\text{surface})$, $\text{O}_2^-(\text{surface})$ and $\text{O}^{2-}(\text{bulk})$] on reduced Ar^+ -bombarded surfaces that had been exposed to oxygen gas, and we found that these oxygen species are formed in three different oxygen-exposed regions.

Annealing Ar^+ -ion-bombarded TiO_2 surfaces in vacuum results in reoxidation of the surface (by diffusion of lattice oxygen atoms from the bulk to the surface) as well as reordering of the surface. The annealing temperature region in which reoxidation occurs ($300^\circ\text{C} \leq T \leq 600^\circ\text{C}$) and the annealing temperature at which ordering takes place

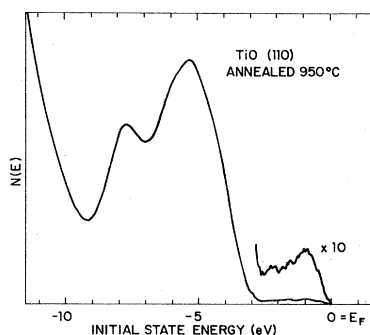


FIG. 21. Photoemission spectrum of an annealed TiO_2 (110) surface. This surface had been annealed at $T = 950^\circ\text{C}$ for 30 min. after Ar^+ bombardment.

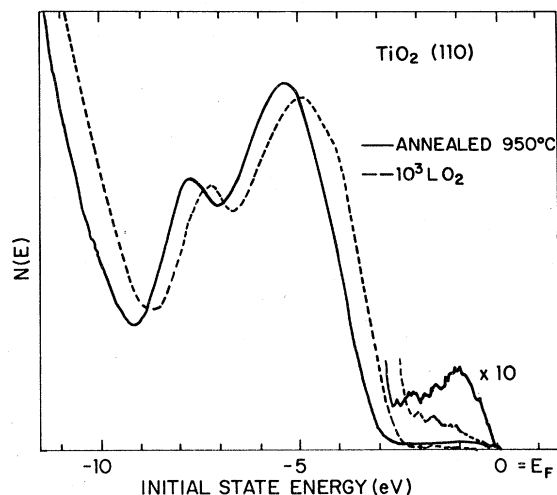


FIG. 22. Photoemission spectra of an annealed TiO_2 (110) surface before and after exposure to 10^3 L of oxygen.

($T = 475^\circ\text{C}$) are the same for both the (001) and (110) surfaces. Furthermore, the gross changes that occur in the valence-band electronic structure of both surfaces when they are annealed are the same and are indicative of decreased titanium coordination of oxygen atoms.

Although the gross annealing behavior of the two surfaces was the same, the detailed behavior of the (001) surface was quite different from that of the (110) as was expected based on one-electron DOS calculations.³ In particular, the (001) surface reconstructs or facets in a complex way when an-

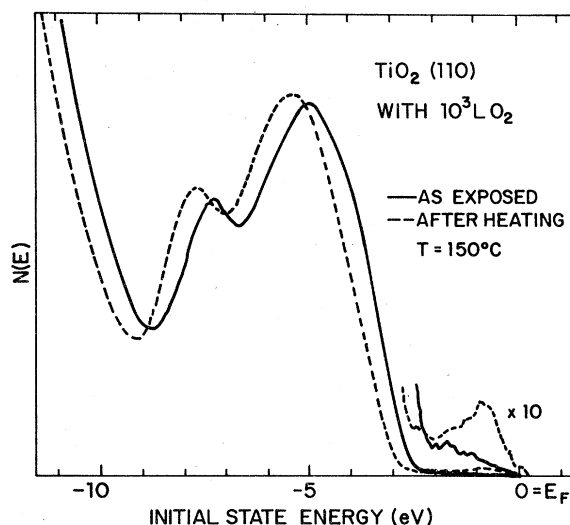


FIG. 23. Photoemission spectra of an annealed TiO_2 (110) surface first exposed to 10^3 L of oxygen and then heated for 30 min. at $T = 150^\circ\text{C}$.

nealed, while the (110) does not reconstruct. The (001) surface undergoes a structural transformation for $T > 900^\circ\text{C}$ (as shown by LEED), while the (110) surface structure is stable. The $\text{O}(2p)$ valence-band UPS spectrum of the (001) surface changes substantially when the structural transformation takes place, and the UPS spectrum of this high-temperature phase can be further altered by heat treatment at $T = 550^\circ\text{C}$. However, the UPS spectrum of the (110) surface of TiO_2 is unaffected by thermal treatment once the surface is completely reoxidized and ordered by annealing at $T \geq 650^\circ\text{C}$.

Furthermore, the oxygen-adsorption behavior of the ordered (001) and (110) surface is different. We identified both strongly bound adsorbed oxygen atoms and weakly bound $\text{O}_2^-(\text{surface})$ on the high-temperature phase of the (001) surface exposed to 10^3 L of O_2 . We identified only weakly bound $\text{O}_2^-(\text{surface})$ on a (110) surface following similar

treatment.

Based on these observations, we conclude that local O-Ti coordination is responsible for the surface band structure and stability of TiO_2 surfaces. In particular, we conclude that the (001) surface of TiO_2 reconstructs to eliminate dangling-bond surface states that arise because of fourfold O-coordinated Ti's on the *unreconstructed* surface. The (110) surface does not reconstruct because there are no fourfold O-coordinated Ti's on this surface.

ACKNOWLEDGMENTS

We would like to thank H. S. Jarrett and T. Wolfram for many helpful and encouraging conversations. The technical help of K. D. Raffell and D. Meinhaldt is appreciated.

*Present address: Savannah River Laboratory, E. I. du Pont de Nemours and Co., Aiken, SC 29801.

¹A. Walker, M. Formenti, P. Meriaudeau, and S. Teichner, *J. Catal.* **50**, 237 (1977); A. H. Boonstra and C. Mutsaers, *J. Phys. Chem.* **79**, 2025 (1975).

²A. Fujishima and K. Honda, *Nature (London)* **238**, 37 (1972); M. S. Wrighton, D. S. Ginley, P. T. Solczanski, A. B. Ellis, D. L. Morse, and A. Linz, *Proc. Nat. Acad. Sci. U. S. A.* **72**, 1518 (1975).

³R. V. Kasowski and R. H. Tait, *Phys. Rev. B* **20**, 5168 (1979).

⁴V. E. Henrich, G. Dresselhaus, and H. J. Zeiger, *Phys. Rev. Lett.* **36**, 1335 (1976).

⁵V. E. Henrich, G. Dresselhaus, and H. J. Zeiger, *J. Vac. Sci. Technol.* **15**, 534 (1978).

⁶V. E. Henrich, G. Dresselhaus, and H. J. Zeiger, *Phys. Rev. B* **17**, 4908 (1978).

⁷Y. W. Chung, W. J. Lo, and G. A. Somorjai, *Surf. Sci.* **64**, 588 (1977); W. J. Lo, Y. W. Chung, and G. A. Somorjai, *ibid.* **71**, 199 (1978).

⁸W. J. Lo and G. A. Somorjai, *Phys. Rev. B* **17**, 4942 (1978).

⁹O. W. Johnson, S. H. Paek, and J. W. DeFord, *J. Appl. Phys.* **46**, 1026 (1975).

¹⁰P. D. Fleischauer and A. B. Chase, *J. Phys. Chem.*

Solids **35**, 1211 (1974).

¹¹D. C. Cronmeyer, *Phys. Rev.* **87**, 876 (1952).

¹²The pronounced peak at -10.6 eV, as noted in Ref. 7, is probably an impurity peak as are the sharp features at -5.1 eV. These features appeared in our data only when we had not baked our vacuum system after opening it to the atmosphere. The locations of these peaks correspond closely to the locations of peaks seen for Ar^+ -ion bombarded TiO_2 surfaces that had been exposed to H_2O . [See V. E. Henrich, G. Dresselhaus, and H. J. Zeiger, *Solid State Commun.* **24**, 623 (1977).]

¹³V. E. Henrich, H. J. Zeiger, and T. B. Reed, *Phys. Rev. B* **17**, 4121 (1978).

¹⁴Electron bombardment of TiO_2 surfaces (Ar^+ -bombarded or annealed) that had been exposed to oxygen gas caused removal of weakly bound oxygen species as shown by the reappearance (or increase in amplitude) of the Ti^{+3} (3d) UPS peak on these surfaces after Auger analysis. Therefore, it is clear that Auger analysis of the composition of these surfaces would not detect the presence of these oxygen species.

¹⁵P. C. Gravelle, F. Juillet, P. Meriaudeau, and S. J. Teichner, *Faraday Discuss. Chem. Soc.* **52**, 140 (1971).



FIG. 11. LEED pattern from a Phase II TiO_2 (001) surface. This surface had been annealed for 30 min. at $T = 750^\circ\text{C}$ following Ar^+ bombardment.

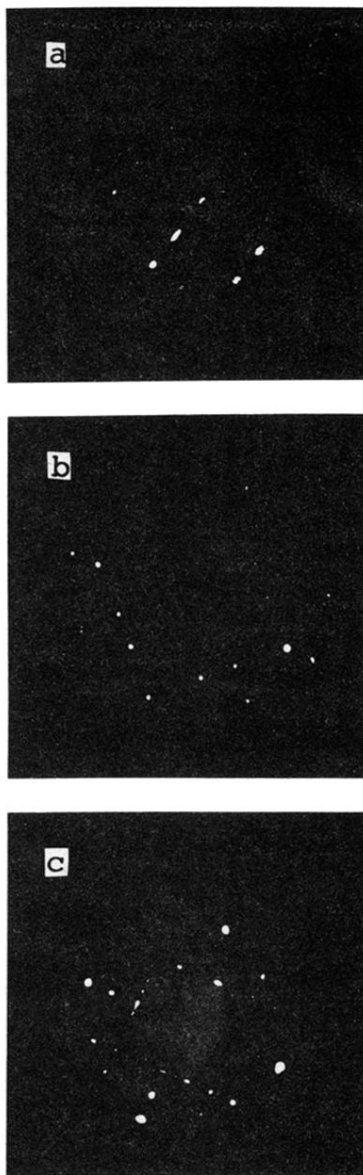


FIG. 14. LEED patterns for a Phase II TiO_2 (001) surface. The surface had been annealed at $T = 1050^\circ\text{C}$ for 30 min. (a) $E_p = 19\text{V}$, (b) $E_p = 28\text{ V}$, and (c) $E_p = 43\text{ V}$.



FIG. 20. LEED pattern of a TiO_2 (110) surface that had been annealed at $T = 950^\circ\text{C}$ for 30 min. after Ar^+ bombardment.